Macromolecules

ARTICLE

pubs.acs.org/Macromolecules

The Kinetics of Gel Formation for PEO−PPO−PEO Triblock Copolymer Solutions and the Effects of Added Methylparaben

Norman A. K. Meznarich and Brian J. Love*

Department of Materials Science and Engineering, University of Michigan, 2300 Hayward Street, Ann Arbor, Michigan 48109, United States

ABSTRACT: We have measured the thermophysical properties of a series of amphiphilic copolymeric F127 solutions (10−30% w/w) as they have been heated between 15 and 65 °C using ramp rates of 0.1−10 °C/min to study their kinetics of gelation using rheology and DSC. DLS was used to further characterize micelle size. A complementary set of experiments was conducted adding methylparaben, a model pharmaceutical, in order to investigate how the added solute affected the gelation properties of the system. From the rheology results, our use of power law analysis to determine the gelation temperature (T_{gel}) indicates that T_{gel} increases at higher temperature ramp rates as compared to the equilibrium or near-equilibrium ramp condition. An alternative analysis using a log-Boltzmann sigmoidal fitting shows a decreased characteristic gelation time for higher ramp rates as well. The gel temperature decreases with increasing F127 concentration, which is expected. The ordering of the micelles is nearly athermic, however, we identified the secondary ordering peak at higher F127 concentrations. DLS measurements showed an increase in micelle monodispersity in the presence of methylparaben, providing one possible explanation for the resultant rheological behavior. These observations suggest that a more refined microstructural evaluation of triblock copolymer dynamic ordering will resolve both the driving force and kinetics of association of amphiphilic copolymers in solution.

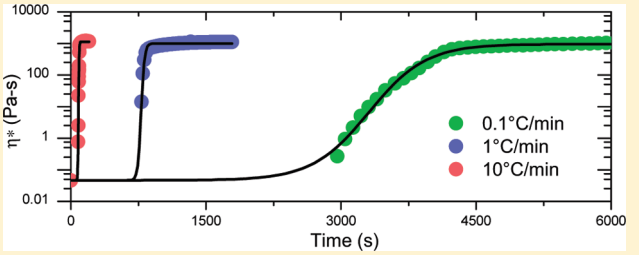

INTRODUCTION

Researchers have harnessed the thermoreversibility of aqueous dispersions of PEO−PPO−PEO triblock copolymers (commercially known as Pluronics) as drug-delivery vehicles and as formulated injectables. The mechanism for the gel formation is mainly attributed to the close packing and ordering of Pluronic micelles.[1−3] As the temperature of Pluronic solutions is increased, the dissolved polymer micellizes in order to minimize the increasing enthalpic penalty arising from the association of the relatively hydrophobic PPO center block with the aqueous solvent. As the temperature is further increased, the micelles grow in size, and the volume fraction that they occupy in solution grows until the micelle shells, composed of PEO segments, interact with those of neighboring micelles. This repulsive interaction is the driving force for the arrangement of the micelles into ordered structures. The relative lengths of the hydrophobic center block and hydrophilic arms regulate the driving force for the structural evolution. For Pluronic F127 ($PEO_{99}PPO_{65}PEO_{99}$), it has been determined that the gel phase consists of micelles arranged in a cubic packing pattern,[4] although altering the block lengths of the interior and the terminal blocks also affects the critical micelle temperature and concentration. While the thermodynamics of these phase transitions and the corresponding phase boundaries have been studied extensively,[1−3,5−7] the kinetics of the gel transition are less well-known.

Separately, it is known that additives can alter the chemical potential enough to change the driving force for micellization.[8−12] Shear can also enhance the ordering of F127 micelles.[13−15] The methods to probe the phase and structure behavior of these systems include rheological and calorimetric tools, probes of bonding[16] and scattering techniques (SANS, SAXS) with the primary structural organizations being observed either as FCC or BCC structures.[17] Other Pluronic systems have also been identified to use the BCC or HCP arrangements.[8]

Pluronic mixtures have been increasingly considered as "functional" fluids leveraging their response as formulations that undergo well-defined and planned structural rearrangements from some active change in equilibrium. Recent efforts have been probing the interaction between certain specific clays (Laponites) and Pluronic mixtures.[18,19] These systems symbiotically reorganize in the presence of light when formulated with photoacid generators through the photoinduced changes in pH and other characteristics which are thought to direct the copolymer into rearranging,[20] which has led to new directions of functional nanocomposite formation.

Continuing needs associated with the kinetics of gelation relate to the development of mathematical models to describe the dynamics of structural evolution. These functional changes such as rheological advancement, gelation, or some other measured observation can occur with time as well. Lam et al.[21] developed a model describing micelle interactions in Pluronics. They concluded that micelle growth occurs primarily via micelle

Received: February 9, 2011
Revised: March 23, 2011
Published: April 05, 2011

coalescence in a process similar to Ostwald ripening. This investigation is a promising start, however, ambiguity still exists in correlating some of the predicted phenomena with observed results, or considering the presence of dissolved solutes. We have been developing kinetic models to describe gelation and have probed the breadth of phenomenological models tied to a range of reactive systems including epoxies[22−24] and acrylates.[25]

Here, we report on the thermophysical properties of a series of amphiphilic copolymeric F127 solutions (10−30% w/w) as they have been heated through the gelation temperature using ramp rates of 0.1−10 °C/min to by both rheology and DSC. We have compared both neat solutions and those including methylparaben (MP) as a drug mimic to modulate the formulation.

■ MATERIALS AND METHODS

Sample Preparation. Pluronic F127 was obtained from Sigma-Aldrich (St. Louis, MO) and used as received. Solutions ranging from 10% to 30% were prepared as described previously.[26] Briefly, weighed amounts of F127 were added to deionized water and stirred. The solutions were refrigerated overnight in order to fully solubilize the F127 and to let any foam buildup dissipate. Occasionally repeated mix/cool cycles were needed to completely solubilize the added F127, particularly for the higher concentrations.

Methylparaben was also obtained from Sigma-Aldrich and solutions were prepared using the method of Sharma et al.[27] MP was added to a 10% F127 solution and stirred until a saturated solution was achieved (approximately 2%). A saturated concentration was chosen assuming that a higher concentration of additive would affect a greater change, and therefore maximizing the amount of additive present would maximize any rheological response. The solution was then filtered through a vacuum filter and weighed amounts of F127 added to aliquots of the MP saturated 10% F127 solution until the desired final F127 concentration was achieved. All F127 and F127 + MP solutions were stored at 4 °C prior to use. A solution containing 1% added MP was prepared using the same method, and diluted to create a series of solutions containing 0.1% to 1% MP.

Rheometry. Rheometry was carried out on a TA Instruments (New Castle, DE) ARES rheometer in dynamic oscillatory mode using parallel plate geometry (diameter 25 mm and gap size between 1 and 1.5 mm). A frequency of 10 rad/s and a strain of 1% were used in the temperature ramp tests. These measurement parameters were chosen to both minimize the applied strain to the sample and to ensure the samples were tested in the linear viscoelastic region. Our chosen parameters are within or near the parameters chosen by others.[1,7,28] Temperature control was achieved using a Peltier accessory, giving both above ambient and subambient thermal control. Ramp rate tests were typically carried out between 15 and 65 °C, ending with a 10-min incubation at 65 °C at the end of each test to allow for any temperature-lagging processes to complete. At higher F127 concentrations, the gel transition occurs near or below 15 °C and thus lower starting temperatures were used. For the 0.1 °C/min ramp rate, a 10 deg window surrounding the gelation temperature was used to capture the transition at a slow rate, but the remainder of the sweep was carried out at 1 °C/min to speed up the remainder of the test and minimize sample evaporation. Data was collected at sampling frequencies between 0.1 and 1 Hz for all heating tests. Initial viscosity measurements were performed using a dynamic frequency sweep at the starting temperature for each F127 concentration. For the initial viscosity measurements, the frequency step increment was 0.05 rad/s.

Power Law Analysis on Rheometry Data. Power law analysis was used to quantify T_{gel} from the rheometer data. Then $\log(\eta)$ vs $\log(t)$ was plotted, and the linearly increasing region of viscosity was identified, an example of which is shown in Figure 1. The experimentally measured initial viscosity was used in conjunction with the linear fit equation to calculate the time of gelation as the intersection of the two lines. Finally, the time of gelation was correlated to the temperature of the system by matching the calculated time to the raw data temperature readout. Figure 1 illustrates an example data set analyzed using this method.

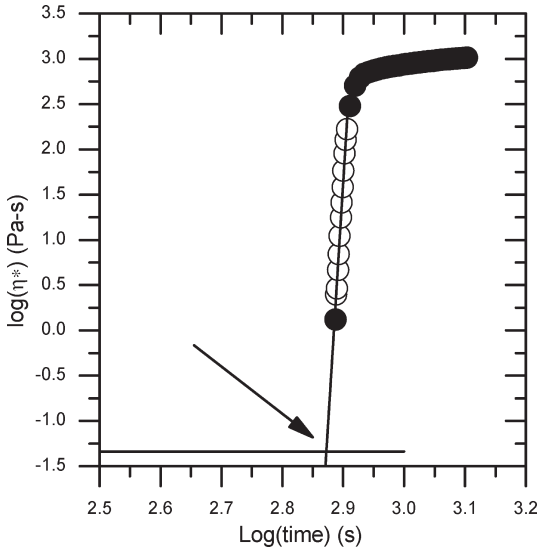

Figure 1. Power law analysis applied to a sample data set of 20% F127 heated at 1 °C/min. The open circles indicate the region in which the data was used to fit the trendline, which has been extrapolated backward and intercepted with the initial viscosity baseline value (arrow). The temperature at this time is defined as T_{gel}. For clarity, the pregelation data has been excluded (as was done for the analysis) and the number of data points plotted here was reduced compared to the actual data used in the analysis.

Log−Boltzmann Sigmoid Modeling. The log−Boltzmann sigmoid model was also used to determine a characteristic gelation time describing the maximum rate of gelation using Origin (version 8). Eq 1 shows the fitting model

$$\log \eta^*(t) = \log(\eta_f) + \frac{\log(\eta_0) - \log(\eta_f)}{(1 + e^{t - t_0/\Delta t})} \quad (1)$$

where the inflection time, t_0, is defined as the time when the viscosity of the solution is halfway between the initial and final logarithmic viscosities. The slope of the sigmoid curve at the inflection time is described in eq 2.

$$\frac{d[\log(\eta_{t_0})]}{dt} = \frac{\log(\eta_f) - \log(\eta_0)}{4\Delta t} \quad (2)$$

The total gel time can be interpreted as $4\Delta t$, which is the time it takes to transition from the initial to the final viscosity value. As Δt decreases, so does the time it takes to reach maximum viscosity, and thus can be used to compare the rate at which different F127 formulations gel. Data prior to the onset of gelation was excluded, and the initial viscosity from the frequency sweep experiments substituted in for η_0. Automatic fitting of the sigmoid curve did not always provide the best fit. When the shape of the viscosity curve did not match well to automatic fitting, the parameters were adjusted to ensure that the slope of the rising portion of the viscosity curve was accurately captured by the Δt parameter in the fitting model.

Differential Scanning Calorimetry. DSC was performed on a TA Instruments Q2000 DSC. Samples were loaded in hermetically sealed aluminum T-zero pans and temperature ramps were carried out using generally the same heating rates and temperature end points as

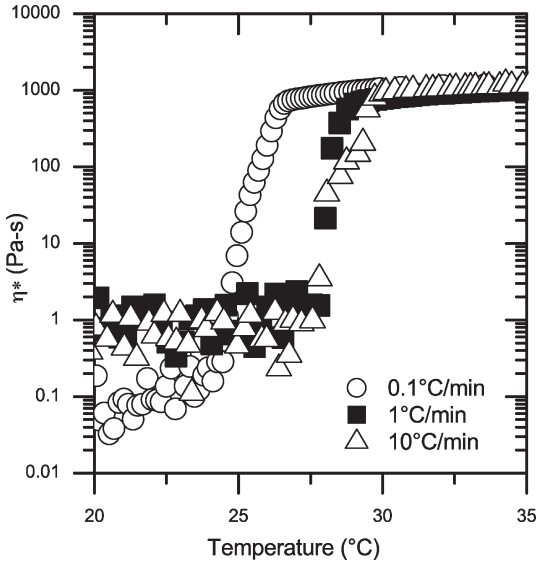

Figure 2. Viscosity vs temperature for 20% F127. Three different heating rates are shown indicating the effect dT/dt has on T_{gel}.

with rheometry. In order to maintain a steady heat flow baseline, a constant ramp rate was needed throughout the duration of each run. Experiments were conducted at near equilibrium heating rates (0.1 °C/min) and as high as 10 °C/min. The onset and peak temperatures, and enthalpies of transition were determined using the TA Instruments Universal Analysis software package (version 4.5.0.5).

Dynamic Light Scattering. DLS experiments were conducted on an ALV compact goniometer system (Model ALV/SP-125, Langen, Germany) using an ALV/SO-SIPD photon detector. An Innova 70C argon ion laser (Coherent Inc., Santa Clara, CA) with a wavelength of 488 nm and a power of 200 mA was used as the light source. Samples of 1% F127 with and without 0.1% MP were gently filtered through a 0.22 μm filter and degassed under vacuum prior to measurement in the DLS. Data was collected for 1 min per reading after equilibration at 30 °C. Scattering angles between 40 and 90° were used, collected every 10 deg. The ALV fitting software uses a constrained regularized method (CONTIN)[29] to obtain particle size distributions from the autocorrelation functions.

RESULTS

Heating Rate Influences Gelation Temperature. Figure 2 shows a comparison of three rheometry experiments carried out at different heating rates at a fixed F127 concentration. A higher T_{gel} for increasing dT/dt was observed across all concentrations tested, although a greater influence on gelation temperature was encountered at lower F127 concentrations. As the heating rate rose from 0.1 to 1 °C/min, the difference was most noticeable. A power law analysis quantifying the F127 gelation temperatures for both neat and MP saturated mixtures are presented in Table 1.

Heating Rate Influences Gelation Time. A log−Boltzmann sigmoid model was used to characterize Δt was used and the results compiled in Table 2. Globally, Δt decreases with increasing heating rate and higher F127 concentration. Increasing dT/dt also had an influence on Δt. Figure 3 shows raw data from a 20% F127 solution heated at three different dT/dt conditions, along with the sigmoid fitting for each curve. For F127 concentrations below 20%, the final viscosity value for the varying dT/dt was also different, indicating that heating rate has an effect on the final viscosity of the gel as well. A wider thermal influence on Δt was

Table 1. Gelation Temperature As Analyzed by Power Law Analysis[a]

	F127 concentration (%)	0.1 °C/min	1 °C/min	10 °C/min
Neat F127	10	44.9 ± 1.3	47.2 ± 1.8*	58.5 ± 1.8
	15	30.0 ± 0.1	31.5 ± 0.3	50.5 ± 0.4
	20	23.9 ± 0.1	27.5 ± 0.3	26.6 ± 0.4
	25	19.8 ± 0.1	22.2 ± 0.1	20.0 ± 0.3
	30	17.0 ± 0.1	19.3 ± 0.0	19.3 ± 0.7
F127 + MP	10	46.9 ± 1.6	33.6 ± 1.0*	63.8 ± 2.0
	15	25.4 ± 0.4	30.0 ± 1.9	46.6 ± 0.8
	20	12.0 ± 0.0	12.4 ± 0.1	12.4 ± 0.3
	25	9.9 ± 0.0	10.3 ± 0.1	10.8 ± 0.2
	30	8.1 ± 0.1	8.3 ± 0.01	8.9 ± 0.5

[a] The asterisks indicate data that was collected using a smaller gap dimension of ~0.6 mm because the tests ran at larger gaps resulted in a lack of identifiable gelation.

experienced at lower F127 concentrations; however, the rapidity of gelation at high heating rates and high F127 concentrations made precise quantification of Δt difficult.

Addition of Methylparaben Influences the Gel Transition. As reported previously,[12,27,30,31] the micellization and gelation behavior of Pluronics is modified by the presence of dissolved solutes. Figure 4 shows the difference in gelation temperature for neat F127 compared to F127 + MP. Adding saturated MP lowered T_{gel} and Δt at or above 15% F127. The positive difference value shown at 10 °C/min and 10% F127 might be a result of thermal lag or sample dehydration influencing the system, where the temperature of the sample had already reached its maximum before gelation was complete, skewing the results toward a positive value. We will address this point further in the discussion. At high heating rates, there is a pronounced lowering of T_{gel} when compared to neat F127. There is also some degree of concentration dependence on the lowering of T_{gel}, with the intermediate concentrations of F127 being the most sensitive to the addition of MP. Sharma et al.[27] reported a lowering in T_{gel} upon adding MP on the order of 20 °C for their tested F127 concentrations (14−30%). Their results, however, did not consider the effect of heating rates, since they measured T_{gel} using a tube inversion method and controlled temperature by immersing their samples in a water bath.

The addition of MP has the effect of decreasing Δt. Figure 5 compares Δt for neat F127 and F127 + MP. Again there is an increased sensitivity to the presence of MP at intermediate F127 concentrations (15−20%). Above 25% F127, adding MP has no effect on Δt that we could measure.

Enthalpy of Micelle Formation vs Micelle Ordering. Figure 6 shows the heat flow vs temperature curves of various F127 concentrations as measured by DSC. This figure highlights the transitional behavior between 6 and 30 °C and shows clear endotherms corresponding to micelle formation in solution at three different concentrations. For higher F127 concentrations (20% or greater), a smaller secondary endotherm (arrow) can also be identified near 15 °C. This smaller peak corresponds to micelle ordering into a quasi-crystalline structure. The enthalpic magnitude of this transition is very small compared to the overall micellization endotherm, but its transition temperature correlates with the gelation temperature sensed by rheometry. While the secondary peak is likely present in all conditions where

Table 2. Gelation Time As Analyzed by Log−Boltzmann Sigmoid Modeling[a]

heating rate (°C/min)	F127 concentration (%)	$\log(\eta_0)$ (Pa-s)	$\log(\eta_f)$ (Pa-s)	t_0 (s)	Δt (s)
0.1	10	−1.87	2.68 ± 0.11	4983 ± 732	283 ± 29
	15	−1.72	2.87 ± 0.08	4217 ± 29	333 ± 58
	20	−1.34	2.98 ± 0.01	3308 ± 11	325 ± 19
	25	−0.98	3.26 ± 0.01	3142 ± 6	89 ± 9
	30	−0.91	3.38 ± 0.00	4774 ± 25	109 ± 1
	10 + MP	−1.91	2.25 ± 0.09	6417 ± 889	300 ± 0
	15 + MP	−1.46	2.43 ± 0.10	1310 ± 340	233 ± 58
	20 + MP	−0.80	3.12 ± 0.01	1786 ± 12	103 ± 6
	25 + MP	−0.69	3.27 ± 0.08	3447 ± 12	105 ± 24
	30 + MP	−0.50	3.37 ± 0.01	2282 ± 20	87 ± 6
1	10*	−1.87	2.25 ± 0.05	2932 ± 39	253 ± 17
	15	−1.72	1.67 ± 0.02	1181 ± 33	129 ± 10
	20	−1.34	3.00 ± 0.01	783 ± 5	18 ± 1
	25	−0.98	3.25 ± 0.00	457 ± 2	11 ± 3
	30	−0.91	3.37 ± 0.01	874 ± 3	6 ± 2
	10 + MP*	−1.91	2.27 ± 0.06	2178 ± 28	244 ± 9
	15 + MP	−1.46	2.05 ± 0.00	1015 ± 123	52 ± 8
	20 + MP	−0.80	3.17 ± 0.03	366 ± 178	3 ± 0
	25 + MP	−0.69	3.36 ± 0.01	580 ± 1	5 ± 1
	30 + MP	−0.50	3.44 ± 0.02	462 ± 0	7 ± 1
10	10	−1.87	1.73 ± 0.07	411 ± 11	78 ± 1
	15	−1.72	1.80 ± 0.04	284 ± 20	35 ± 2
	20	−1.34	3.06 ± 0.01	84 ± 1	4 ± 0
	25	−0.98	3.31 ± 0.01	46 ± 2	4 ± 1
	30	−0.91	3.43 ± 0.01	102 ± 3	3 ± 1
	10 + MP	−1.91	1.30 ± 0.05	481 ± 12	54 ± 4
	15 + MP	−1.46	1.71 ± 0.14	258 ± 13	30 ± 5
	20 + MP	−0.80	3.15 ± 0.01	60 ± 2	3 ± 0
	25 + MP	−0.69	3.34 ± 0.00	73 ± 2	4 ± 1
	30 + MP	−0.50	3.45 ± 0.01	60 ± 3	3 ± 0

[a] The results marked with asterisks indicate data that was collected using a smaller gap dimension of ~0.6 mm.

gelation (the ordering of micelles) occurred, it was not resolvable at all concentrations measured by DSC.

Addition of Methylparaben Suppresses Micellization Endotherm. Adding MP to F127 also suppresses the endotherm associated with F127 micellization. Figure 7 shows representative heat flow curves for 10% F127 with increasing amounts of added MP. The micellization endotherm is suppressed and moves toward lower temperatures. We believe that micellization and ordering still occur for the saturated MP solutions used in the rheometry experiments, as the results clearly indicate gelation for the F127 + MP solutions. Further consideration on this finding follows.

Micelle Monodispersity Increases with Added Methylparaben. DLS results, shown in Figure 8, indicate no significant difference in micelle size at the higher scattering angles (70° or greater). At lower angles, however, the samples containing MP show a decreased micelle radius as compared to the neat F127 samples. This result is not immediately clear to us, as the micelle radius obtained via DLS should not depend on the scattering angle. When considering the high scattering angles, however, our results are comparable to those published previously, all of whom reported their micelle radii at a scattering angle of 90°.[6,32,33]

Micelle monodispersity increased under certain circumstances as a result of added MP. Figure 9 shows a plot depicting representative radius intensity distributions for both a neat F127 and F127 + MP sample at a scattering angle of 70°. This trend was generally conserved over the range of collected scattering angles, but most pronounced at 70°. This observation coincides with that of Sharma et al.[34] who also noted an increase in monodispersity as a result of added MP, based on their analysis of SANS data.

DISCUSSION

Prior work relating to the phase behavior of amphiphilic copolymeric solutions has focused mainly on the thermodynamic equilibrium states of the phase diagram.[2,3,30,35] We have shown here that kinetics also affects the gelation behavior in a systematic way between 15 and 30% F127. Higher heating rates correlate with a generally higher gelation temperature and a shorter gelation time. We observed complications associated with higher variance in the determination of gel time and gel temperature testing solutions of 10% F127, both with and without MP and an unusual dependence on gap dimension on whether gelation occurs at 1 °C/min. Smaller gaps led to an identified gel formation while gaps similar to those used for other compositions yielded no observed gel in some instances. We attribute this anomalous rheological behavior at 10% F127 to the low propensity of those solutions to gel, and to sample dehydration. 10%

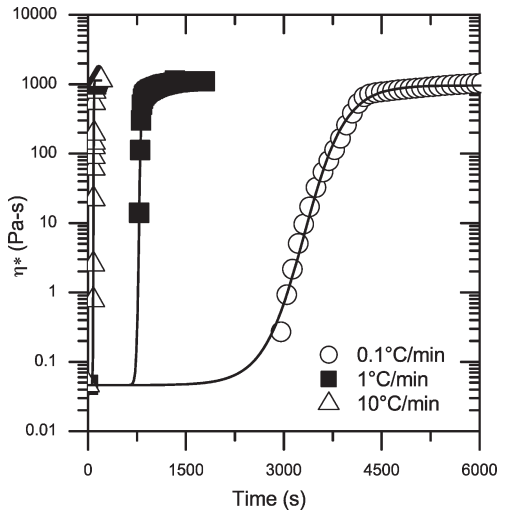

Figure 3. Viscosity vs time for 20% F127. Three different heating rates are shown indicating the effect dT/dt has on the rate of gelation, or gelation time. The black line indicates the log-Boltzmann sigmoid fit for each run. For clarity, the number of data points shown here has been reduced in the 1 °C/min and 10 °C/min rates.

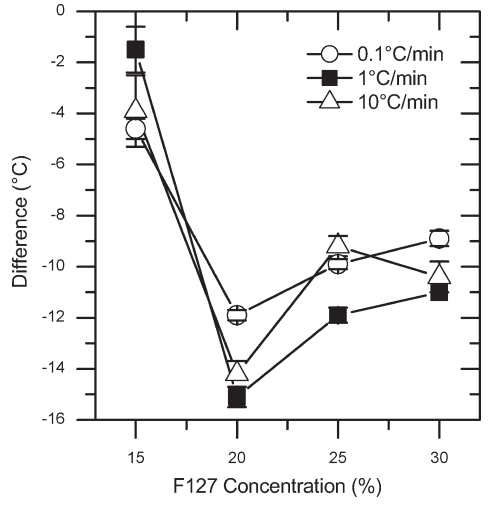

Figure 4. Gelation temperature lowering as a result of adding methylparaben to F127, excluding data at 10%, which we believe is dehydrating prior to gelation.

F127 undergoes gelation at the highest temperatures of the samples we tested, and it is likely that the sample has dehydrated significantly by the time the gelation temperature has been reached. Thus, any rheological response we measured is more likely to be that of the dehydrated residues of the samples and not of the 10% solutions themselves. We experience sample dehydration at all samples, however, with the higher concentrations the gelation temperature is lower, and the gel transition has an opportunity to complete prior to the sample dehydrating.

One explanation for our observed results is that the gelation is related simply to the heating time of our system; that is the faster gelation seen at higher heating rates is simply due to the fact that we reach the maximum temperature in less time. If gelation for F127 were driven solely by thermodynamics, this would be the case. However, in such an instance the gelation time would scale

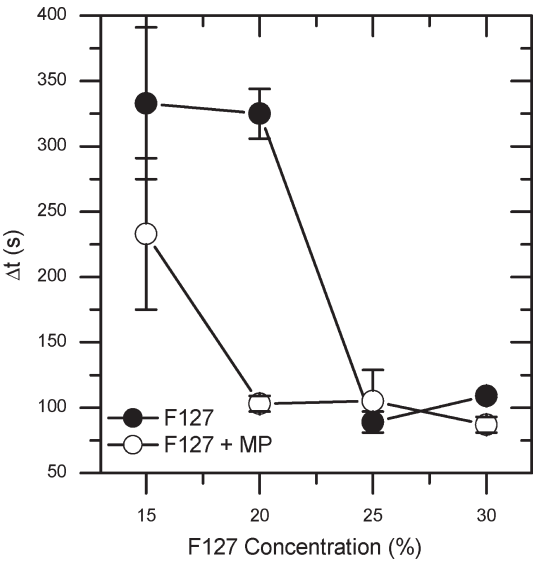

Figure 5. Characteristic gelation time decreases as a result of adding methylparaben to F127, again excluding the data for 10% F127.

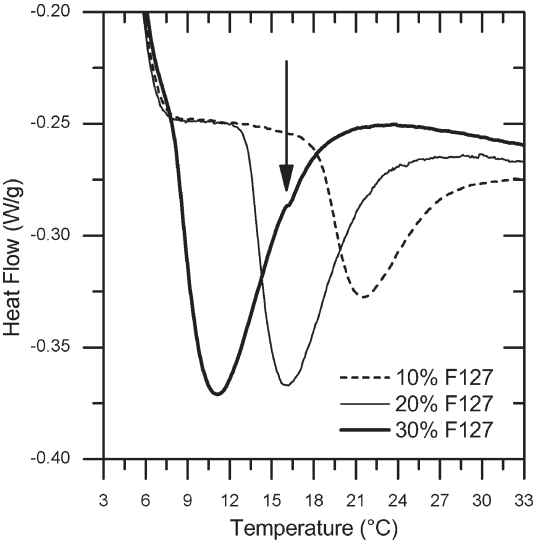

Figure 6. Heat flow curves for various F127 concentrations at a heating rate of 10 °C/min. Curves were offset on the y-axis in order to facilitate comparison. The arrow points toward a second peak corresponding to the formation of the micelle gel.

directly in proportion to the heating rate. The results shown in Table 2 indicate that on average, while the heating rate was changed by a factor of 100 from the lowest to the highest conditions tested, Δt only changes by a factor of 10−30. Therefore, some kinetic factors are present in this system.

There are several methods or criterion by which one can determine a gel point, each producing subtly different results based on the definition of when a solution has converted to the gel state. A brief discussion on gel point determination can be found by Lau et al.[1] Our method for gel point determination was chosen in order to provide a reliable and repeatable baseline by which relative differences in gel temperature or gelation time can be determined. Therefore, subtle differences in the actual gel

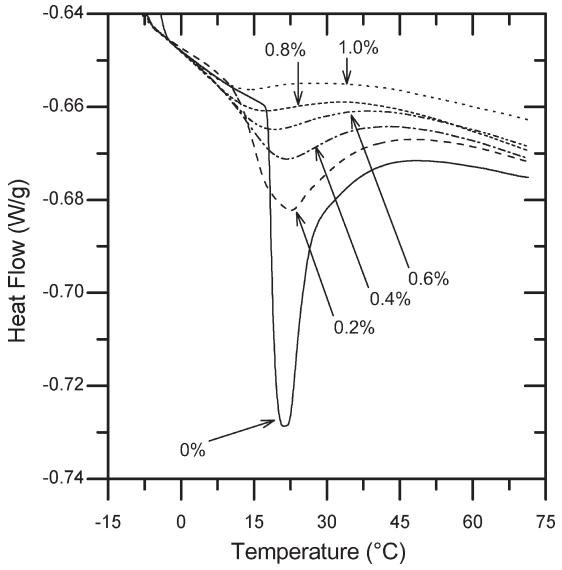

Figure 7. Heat flow vs temperature curve showing suppression of the micellization endotherm upon the addition of MP for 10% F127. The arrows indicate the MP concentration. A large suppression in peak size is seen between 0% and 0.2% MP, with the peak suppressing further and trending toward lower temperatures as more MP is added.

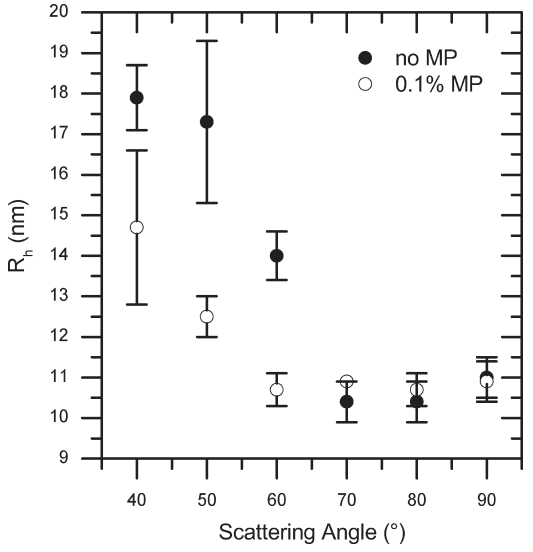

Figure 8. Measured hydrodynamic radius (R_h) as a function of scattering angle. The filled circles indicate 1% F127 solutions and the open circles indicate 1% F127 + 0.1% MP solutions.

temperature exist when comparing our data with related works. These small differences can be reconciled by the different definitions of gel formation used. More importantly to us, identifying the relative differences in gelation behavior between the different heating rates and concentrations are the main focus of our analysis.

The most pronounced trends in the sensitivity of F127 gelation to the addition of MP were found at intermediate F127 concentrations using rheology, seen in Figure 4. At high concentrations (25% F127 or greater), no difference in Δt is observed by adding MP. There are two plausible explanations for

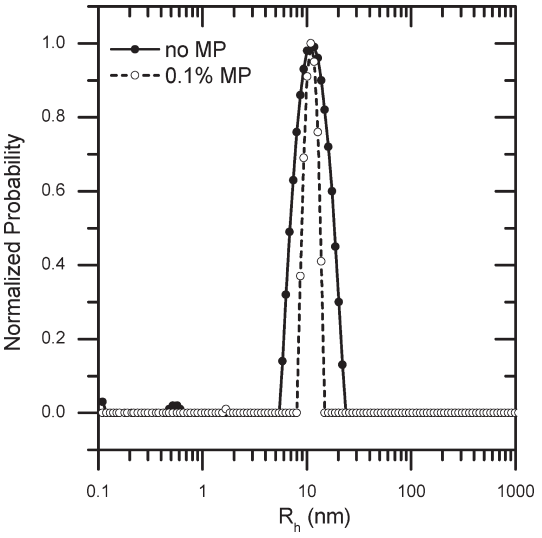

Figure 9. Normalized probability intensity as a function of R_h for two samples, one of 1% F127 and the other 1% F127 + 0.1% MP collected at a 70° scattering angle. The neat F127 sample shows an increased polydispersity compared to the MP-containing sample.

this observation. One possibility is that the driving force to gel is sufficiently high to overwhelm any perturbation induced by the presence of MP. Alternatively, the fast gelation at these high concentrations (occurring over the span of only a few seconds in most circumstances) is near or beyond the resolving limit of the 1 Hz sampling interval used for the rheometry experiments. At the lowest concentrations tested, the presence of MP has no more than a 5 °C difference on T_{gel} as seen in Figure 4. Only at the intermediate concentrations of F127 do we observe facilitated micelle ordering caused by the presence of MP.

Relating to Table 1, increasing F127 concentration led to the expected trend of decreased T_{gel} as interpreted by the power law model. At 15% F127 or higher, adding MP globally suppressed the gelation temperature nominally between 2 and 15 °C. The most pronounced suppression is at concentrations of 20% F127 or greater. This suppression due to the presence of MP is largely independent of the heating rate, although equilibrium heating rates produced the lowest suppression. These findings are consistent with prior work by Sharma et al., who observed similar reduction in T_{gel} when adding MP or other pharmaceutical solutes.[27] It is interesting to note that at 10% F127, the addition of MP produced an increase in measured gelation temperature (Table 1). We have previously discussed the complications we experienced with the gelation of 10% F127 solutions, and variations in T_{gel} can be attributed as much to the irregularity of gel formation at low concentrations as it can to the presence of MP.

The relative nonpolarity of MP leads to one possible explanation for its lowering of the gel temperature. During micelle formation, MP is likely sequestered within the micelle core, possibly acting as a plasticizer and interfering with the packing of F127 center regions. In order to better understand the mechanism by which MP affects the gelation behavior of F127, we looked at the effect that MP had on micelle size. If MP causes an increase in micelle size for a given temperature, it would follow that micelle interaction would occur sooner, at lower temperatures. Our DLS results indicated, however, that there was no measurable difference at high scattering angles whereas lower scattering angles indicated a decrease in micelle size from added MP. We

did observe a general increase in micelle monodispersity as a result of added MP. In theory, DLS measurements should be independent of scattering angle, and we cannot explain why we see an increasing trend in measured micelle size when using lower scattering angles. After searching through previously published literature, we were unable to find prior work showing DLS measurements taken at multiple angles, nor angles other than 90°. Therefore, we were unable to determine whether or not others have seen this angle-dependent discrepancy. However, as noted previously, our measured micelle size of ~11 nm at a 90° collection angle are in agreement with the results published by others using the same angle.[6,32,33] It is possible that this angular dependence suggests the presence of micelle aggregation or interaction in our sample, but micelle−micelle interactions at the measurement temperature (30 °C) and concentration (1% F127) should be minimal. We hope that our observation might lead to a further discussion or study on why the DLS of F127 solutions exhibit this angular dependence, and if this method is valid to characterize F127 micelles in solution.

Sharma et al.[34] noted a decrease in the critical micelle concentration (CMC) for F127 solutions with added MP. They suggested that this decrease in CMC would facilitate micellar assembly. Similar to Sharma's conclusion, we reason that the increased micellar monodispersity facilitates the ordering of micelles, as the quasicrystalline lattice structure would not need to accommodate as many sizing defects. This would explain both the lower gelation temperature and gelation time we observed via rheometry.

The increasingly athermal micellization of F127 + MP is also an unexpected observation. It is not immediately known why this occurs; however, there have been previously reported cases of athermal or near athermal micellization. Kelarakis et al.[36,37] reported on the athermal micellization of ethylene oxide/1,2-butylene oxide diblock copolymers. They concluded that a balance of positive and negative enthalpic contributions to micellization accounted for the near-zero enthalpy of micellization. In their system, it was the positive enthalpy of micellization due to the hydrophobic effect balancing with negative contributions to the enthalpy of micellization arising from the dispersion forces within the micelle core. It is possible that by adding MP, a largely nonpolar molecule with a low solubility in water, either the hydrophobicity or the dispersion interactions for Pluronic F127 is modified, and leads to a reduced enthalpy of micellization. Whether or not this trend is general or can be controlled (reducing or increasing the enthalpy of micellization) by careful selection of the solute is worthy of further consideration. This process could perhaps be manipulated to be slightly exothermic by controlling the composition and concentration of the added solute.

It is important to note that rheology and DSC are observational tools that indirectly examine the structural evolution and changes that control the resultant thermophysical behavior for F127 gels. A logical follow up to these findings are to more directly measure the presence and evolution of intermicellar structure in these solutions using scattering methods such as time-resolved SAXS or SANS. Ideally one would observe the micellar structures as F127 is subjected to variable heating rates, in order to determine if there is a systematic change in the evolution of an ordered micelle network as a result of increased dT/dt or due to the presence of additives. Ultimately this correlation between the structural characteristics and the resulting response might lead toward a unified model describing the effects of interacting micelles in polymeric dispersions.

CONCLUSION

Here we have demonstrated rather clearly that heating rate affects the gelation of aqueous solutions of F127 at concentrations ranging from 15 to 30%. The liquid-gel transition was observed between nominally 15 and 45 °C. The presence of MP lowered the liquid-gel transition of F127 to between 8 and 45 °C. The transition between the liquid and the gel states was also accelerated in the presence of MP. We observed a concentration dependent sensitivity in both the gelation temperature and characteristic gelation time to heating rate by rheometry. Additionally, we observed a progressive suppression of the micellization endotherm with increasing MP concentration by DSC. By DLS, we observed that adding MP had no significant effect on micelle size, and led to generally increased micelle monodispersity. This finding provides one possible explanation for the modification in behavior we observed; that the increased monodispersity facilitates the arrangement of micelles into the quasicrystalline lattice structure. The structural changes taking place here are also proposed and actively being investigated by time-resolved SAXS using controlled heating, in order to resolve what structural evolution, if any, occurs.

AUTHOR INFORMATION

Corresponding Author

*Telephone: 734-763-2013. Fax: +1-734-763-4788. E-mail: bjlove@umich.edu.

ACKNOWLEDGMENT

We would like to thank Amy Gros for her assistance in the data analysis. We also thank the Department of Education's Graduate Assistance in Areas of National Need fellowship for supporting Norman during this work. In addition, we thank the Solomon Research Group at the University of Michigan for the use of their DLS system, and for their help in obtaining those results.

REFERENCES

(1) Lau, B.; Wang, Q.; Sun, W.; Li, L. *J. Polym. Sci. Polym. Phys.* **2004**, *42*, 2014–2025.

(2) Wanka, G.; Hoffmann, H.; Ulbricht, W. *Colloid Polym. Sci.* **1990**, *268*, 101–117.

(3) Wanka, G.; Hoffmann, H.; Ulbricht, W. *Macromolecules* **1994**, *27*, 4145–4159.

(4) Mortensen, K.; Talmon, Y. *Macromolecules* **1995**, *28*, 8829–8834.

(5) Barba, A. A.; d'Amore, M.; Grassi, M.; Chirico, S.; Lamberti, G.; Titomanlio, G. *J. Appl. Polym. Sci.* **2009**, *114*, 688–695.

(6) Gentile, L.; De Luca, G.; Antunes, F. E.; Rossi, C. O.; Ranieri, G. A. *Appl. Rheol.* **2010**, *20*, U10–U18.

(7) Trong, L. C. P.; Djabourov, M.; Ponton, A. *J. Colloid Interface Sci.* **2008**, *328*, 278–287.

(8) Artzner, F.; Geiger, S.; Olivier, A.; Allais, C.; Finet, S.; Agnely, F. *Langmuir* **2007**, *23*, 5085–5092.

(9) Chaibundit, C.; Ricardo, N. M. P. S.; Ricardo, N. M. P. S.; Costa, F. d. M. L. L.; Wong, M. G. P.; Hermida-Merino, D.; Rodriguez-Perez, J.; Hamley, I. W.; Yeates, S. G.; Booth, C. *Langmuir* **2008**, *24*, 12260–12266.

(10) Chaibundit, C.; Ricardo, N. M. P. S.; Ricardo, N. M. P. S.; O'Driscoll, B. M. D.; Hamley, I. W.; Yeates, S. G.; Booth, C. *Langmuir* **2009**, *25*, 13776–13783.

(11) Pozzo, D. C.; Walker, L. M. *Colloids Surf., A* **2007**, *294*, 117–129.

(12) Wu, Y.; Sprik, R.; Poon, W.; Eiser, E. *J. Phys.—Condens. Matter* **2006**, *18*, 4461–4470.

(13) Habas, J.; Pavie, E.; Lapp, A.; Peyrelasse, J. *J. Rheol.* **2004**, *48*, 1–21.
(14) Jiang, J.; Burger, C.; Li, C.; Li, J.; Lin, M. Y.; Colby, R. H.; Rafailovich, M. H.; Sokolov, J. C. *Macromolecules* **2007**, *40*, 4016–4022.
(15) Newby, G. E.; Hamley, I. W.; King, S. M.; Martin, C. M.; Terrill, N. J. *J. Colloid Interface Sci.* **2009**, *329*, 54–61.
(16) Lee, S.-Y.; Lee, S.; Youn, I.-C.; Yi, D. K.; Lim, Y. T.; Chung, B. H.; Leary, J. F.; Kwon, I. C.; Kim, K.; Choi, K. *Chem.—Eur. J.* **2009**, *15*, 6103–6106.
(17) Mortensen, K.; Batsberg, W.; Hvidt, S. *Macromolecules* **2008**, *41*, 1720–1727.
(18) Boucenna, I.; Royon, L.; Colinart, P. *J. Therm. Anal. Calorim.* **2009**, *98*, 119–123.
(19) Sormana, J.-L.; Chattopadhyay, S.; Meredith, J. C. *J. Nanomater* **2008**, 869354.
(20) Sun, K.; Kumar, R.; Falvey, D. E.; Raghavan, S. R. *J. Am. Chem. Soc.* **2009**, *131*, 7135–7141.
(21) Lam, Y.; Goldbeck-Wood, G. *Polymer* **2003**, *44*, 3593–3605.
(22) Love, B. J.; Teyssandier, F.; Sun, Y. Y.; Wong, C. P. *Macromol. Mater. Eng.* **2008**, *293*, 832–835.
(23) Teyssandier, F.; Sun, Y. Y.; Wong, C. P.; Love, B. J. *Macromol. Mater. Eng.* **2008**, *293*, 828–831.
(24) Teyssandier, F.; Ivankovic, M.; Love, B. J. *J. Appl. Polym. Sci.* **2010**, *115*, 1671–1674.
(25) Love, B. J.; Piguet-Ruinet, F.; Teyssandier, F. *J. Polym. Sci., Polym. Phys.* **2008**, *46*, 2319–2325.
(26) Schmolka, I. R. *J. Biomed. Mater. Res.* **1972**, *6*, 571–582.
(27) Sharma, P. K.; Reilly, M. J.; Bhatia, S. K.; Sakhitab, N.; Archambault, J. D.; Bhatia, S. R. *Colloids Surf., B* **2008**, *63*, 229–235.
(28) Norman, A.; Fairclough, J.; Mai, S.; Ryan, A. *J. Macromol. Sci. Phys.* **2004**, *B43*, 71–93.
(29) Provencher, S. W. *Comput. Phys. Commun.* **1982**, *27*, 229–242.
(30) Malmsten, M.; Lindman, B. *Macromolecules* **1992**, *25*, 5440–5445.
(31) Scherlund, M.; Brodin, A.; Malmsten, M. *Int. J. Pharm.* **2000**, *211*, 37–49.
(32) Chaibundit, C.; Ricardo, N. M. P. S.; Costa, V. d. M. L. L.; Yeates, S. G.; Booth, C. *Langmuir* **2007**, *23*, 9229–9236.
(33) Wu, C.; Liu, T.; Chu, B.; Schneider, D.; Graziano, V. *Macromolecules* **1997**, *30*, 4574–4583.
(34) Sharma, P. K.; Reilly, M. J.; Jones, D. N.; Robinson, P. M.; Bhatia, S. R. *Colloids Surf., B* **2008**, *61*, 53–60.
(35) Yu, G. E.; Deng, Y. L.; Dalton, S.; Wang, Q. G.; Attwood, D.; Price, C.; Booth, C. *J. Chem. Soc., Faraday Trans.* **1992**, *88*, 2537–2544.
(36) Kelarakis, A.; Havredaki, V.; Yu, G.; Derici, L.; Booth, C. *Macromolecules* **1998**, *31*, 944–946.
(37) Kelarakis, A.; Havredaki, V.; Rekatas, C.; Booth, C. *Phys. Chem. Chem. Phys.* **2001**, *3*, 5550–5552.